HHS Public Access

Author manuscript

J Control Release. Author manuscript; available in PMC 2016 March 28.

Published in final edited form as:

J Control Release. 2015 March 28; 202: 40–48. doi:10.1016/j.jconrel.2015.01.031.

Chemoradiation Therapy using Cyclopamine-Loaded Liquid-Lipid Nanoparticles and Lutetium-177-Labeled Core-Crosslinked Polymeric Micelles

Jian You[a,1,†], **Jun Zhao**[a,†], **Xiaoxia Wen**[a], **Chunhui Wu**[a,2], **Qian Huang**[a], **Fada Guan**[b], **Richard Wu**[b], **Dong Liang**[c], and **Chun Li**[a]

[a]Department of Cancer Systems Imaging, The University of Texas MD Anderson Cancer Center, 1515 Holcombe Blvd., Houston, TX 77030

[b]Department of Radiation Physics, The University of Texas MD Anderson Cancer Center, 1515 Holcombe Blvd., Houston, TX 77030

[c]Department of Pharmaceutical Sciences, College of Pharmacy and Health Sciences, Texas Southern University, 3100 Cleburne Street, Houston, TX 77004

1. Introduction

The Hedgehog pathway is an essential signaling pathway that regulates tumor cell growth in addition to the development of embryonic tissues and the homeostasis of adult stem cells [1]. During activation, Hedgehog ligands (Sonic, Indian, or Desert) bind to transmembrane protein Patched (Ptch1) and relieve its inhibition of Smoothened. The subsequent cascade of events leads to translocation of transcription factor Gli1 into the nucleus. Nuclear Gli1 activates a number of target genes that are involved in cell proliferation and angiogenesis.

Aberrant activation of the Hedgehog pathway is frequently observed in carcinoma tissues. Immunostaining of specimens collected from breast cancer patients revealed overexpression of Sonic Hedgehog, Ptch1, and Gli1 in primary carcinoma but no detectable levels of these proteins in adjacent normal tissue [2]. Hedgehog components were expressed strongly in pancreatic precursor and invasive lesions but not in normal pancreatic ductal epithelium [3]. Similar results were reported in other cancer types, including esophageal, lung, brain, and prostate cancers [4–7].

Blockade of the Hedgehog pathway with inhibitors induces significant antitumor effects [8, 9]. One Hedgehog pathway inhibitor, cyclopamine (CPA), is a potent inhibitor of Smoothened, a seven-transmembrane protein downstream of Ptch1 and upstream of Gli1 [10]. CPA shows promising properties, including prevention of metastasis, disruption of tumor stroma, and depletion of cancer stem cells [11]. However, CPA is insoluble in water

Corresponding Author: Chun Li, Ph.D., Department of Cancer Systems Imaging, The University of Texas MD Anderson Cancer Center, 1515 Holcombe Blvd., Houston, TX 77030, Tel: (+1)713-792-5182, Fax: (+1)713-794-5456, cli@mdanderson.org.
[1]Current address: College of Pharmaceutical Sciences, Zhejiang University, Hangzhou 310058, China
[2]Current address: Department of Biophysics, University of Electronic Science and Technology of China, Chengdu, Sichuan 610054, China
[†]These authors contributed equally to the paper.

and thus not suitable for clinical translation. Several nanoformulations using polymeric micelles or polymer conjugate have been developed to increase the solubility of CPA in water [12–14].

CPA has also been used in combination with other therapeutic modalities [15, 16] and was found to enhance the tumor response to ionizing radiation [17]. Ionizing radiation is widely used in cancer treatment, especially the treatment of inoperable tumors. Since whole-body irradiation causes excessive damage to healthy tissues, techniques have been developed to target radiation to tumor regions; these techniques include delivering radiation internally by using radioisotopes conjugated to tumor-targeting monoclonal antibodies [18, 19] or peptides [20]. Among the radioisotopes that have shown promise for the treatment of solid tumors in clinical trials is lutetium-177 (^{177}Lu). ^{177}Lu emits low β-energy ($E_{\beta max}$ = 497.1 keV), which causes less side effects than those observed with external radiation therapy. ^{177}Lu has a tissue penetration of approximately 2 mm; therefore, it is suitable for treating small tumor cell clusters and micrometastases [18]. Its long half-life (6.7 days) allows the preparation of more sophisticated radioconjugates and is sufficient for purification and transport. In addition to being used for treatment, ^{177}Lu can be used for scintigraphy and dosimetry because it emits γ radiation (208 keV, 11% of all energy emitted) [21]. To date, ^{177}Lu-labeled radiotracers have been evaluated in a number of clinical studies [20, 22].

We hypothesized that CPA encapsulated in liquid-lipid nanoparticles (CPA-LLP) for intravenous injection would have desirable pharmacokinetic properties and substantial anticancer efficacy. We further hypothesized that CPA-LLP would enhance the response of tumor cells to ^{177}Lu conjugated to core-crosslinked polymeric micelles (CCPM-^{177}Lu). We prepared and characterized CPA-LLP and CCPM-^{177}Lu, and evaluated the antitumor activity of CPA-LLP alone and in combination with CCPM-^{177}Lu both *in vitro* and *in vivo* against breast cancer and pancreatic cancer cells. Our data show that the combined chemoradiation therapy is an effective strategy for cancer treatment.

2. Materials and Methods

2.1. Materials and cell lines

CPA was purchased from LKT Laboratories (St Paul, MN). $^{177}LuCl_3$ was purchased from Perkin Elmer (Waltham, MA). Tritium-labeled CPA ([^{3}H]CPA; 1.0 mCi/mg CPA) was obtained from Moravek Biochemicals (Brea, CA). Lecithin E80, lecithin S100, and oleic acid were purchased from Lipoid (Ludwigshafen, Germany). 1-(4-Isothiocyanatobenzyl) diethylenetriaminepentaacetic acid (DTPA-bz-SCN) was obtained from Macrocyclics (Dallas, TX). (3-(4,5-Dimethylthiazol-2-yl)-5-(3-carboxymethoxyphenyl)-2-(4-sulfophenyl)-2H-tetrazolium) (MTS) was purchased from Life Technologies (Carlsbad, CA). All other chemicals were purchased from Sigma-Aldrich (St. Louis, MO) or Fisher Scientific (Pittsburgh, PA).

4T1 murine breast cancer cells and Miapaca-2 human pancreatic ductal adenocarcinoma cells were purchased from American Type Culture Collection (Manassas, VA) and

maintained in Dulbecco modified Eagle medium supplemented with 10% fetal bovine serum and 1% antibiotics. Both cell lines have activated Sonic Hedgehog pathway [10, 23, 24].

2.2. Preparation and characterization of CPA-LLP

CPA (50 mg) and lecithin (3.6 g) were dissolved in 3 mL of ethanol at 50°C, and then olive oil (5.0 g) and oleic acid (0.5 g) were added. The mixture was gently stirred at 50°C until a clear uniform solution was formed. Then ethanol was removed *in vacuo*, and the resultant solution was dispersed into 50 mL of an aqueous solution containing sucrose and L-arginine under stirring. The mixture was homogenized at 10,000 RPM for 5 min and then passed through a Lab Homogenizer M110P (Microfluidics, Westwood, MA) under a pressure of 2000 bars for 10 cycles at room temperature, to give the final product CPA-LLP. CPA-LLP was sterilized by filtering through a 0.22-μm filter, un-encapsulated CPA was also removed during the filtration. For long-term storage, the CPA-LLP suspension was lyophilized and stored at −80°C. In a separate experiment, [^{3}H]CPA was mixed with nonradioactive CPA for the preparation of [^{3}H]CPA-LLP.

For analysis of the content of CPA in CPA-LLP, CPA-LLP suspension was centrifuged at 5,000 RPM for 5 min to remove CPA precipitate. The supernatant was then dissolved in ethanol and sonicated for 5 min to release the encapsulated CPA. After centrifugation at 13,000 RPM for 15 min, the supernatant was analyzed using an Agilent 1100 series high-performance liquid chromatography (Santa Clara, CA). The mobile phase was a mixture of 0.1% TFA (solvent A) and acetonitrile (solvent B), using a gradient (solvent B from 5% to 95% v/v in 30 min). The column was an Agilent C18 column (4.6× 250 mm) with 5-μm particles. The flow rate was 1.0 mL/min, and the detection wavelength was 210 nm. The size of CPA-LLP was measured using dynamic light scattering on a Brookhaven 90 plus particle size analyzer (Holtsville, NY). The morphology of CPA-LLP was analyzed using a JEM 1010 transmission electron microscope (JEOL USA, Inc., Peabody, MA).

2.3. Preparation and characterization of ^{177}Lu-labeled CCPM

CCPM was prepared according to previous reports [25] from the self-assembly and cross-linking of poly[oligo(ethylene glycol) methyl ether methacrylate]$_{30}$-*b*-poly(2-(methacryloyloxy)ethyl 4-oxo-4-(3-(triethoxysilyl)propylamino)butanoate)$_{60}$. The prepared CCPM was then modified with DTPA-bz-SCN to introduce the metal chelator DTPA. After purification, $^{177}LuCl_3$ 1 mCi in 50 μL of sodium acetate buffer (10 mM, pH 5.2) was added to 450 μL of aqueous solution of 20 mg of CCPM-DTPA. The mixture was then incubated at room temperature for 1 hr. Radiolabeling efficiency was analyzed using an instant thin-layer chromatography system (Bioscan IAR-2000 TLC Imaging Scanner, Washington, DC).

2.4. Cell proliferation assay

Cell proliferation was examined using MTS assay. Cells were seeded in 96-well plates and treated with CPA-LLP at various concentrations at 37°C for 96 hr before MTS assay. Cell viability was normalized to that of untreated cells and expressed as mean ± standard error of the mean (SEM) (n = 6).

2.5. Cell clonogenic assay

Cell clonogenic assay was performed as previously reported [26]. To test the effect of CPA-LLP alone, cells were plated at 500 cells per 10-cm plate in growth medium overnight and then treated with CPA-LLP and maintained at 37°C for 10 days. At the end of this 10-day period, formed colonies were fixed with formalin and stained with crystal violet. Colonies consisting of more than 20 cells were counted. To test the radiosensitization effect of CPA-LLP, cells were grown to 80% confluence and then treated with CCPM-^{177}Lu and/or CPA-LLP at 37°C for 24 hr. After washing steps, cells were detached into single-cell suspension and plated at 1000 cells per 10-cm plate. Formed colonies were fixed, stained, and counted as described above. All experiments were performed in 4 replicates.

2.6. Establishment of tumor xenografts in mice

All animal studies were approved by the Institutional Animal Care and Use Committee of The University of Texas MD Anderson Cancer Center and were carried out in accordance with institutional guidelines. Subcutaneous tumor xenografts were established by injecting cell suspensions (5×10^6 cells for 4T1 cells; 1×10^7 cells for Miapaca-2 cells) into the right flanks of Nu/Nu mice (Charles River, Wilmington, MA).

2.7. Pharmacokinetic and biodistribution studies

For pharmacokinetic studies, Balb/c mice (Charles River) were injected intravenously with 20 μCi of [^{3}H]CPA-LLP. At predetermined intervals, blood samples were taken from the tail vein; weighed; solubilized in 1 mL of scintillation-counting-compatible Soluene-350 (Perkin Elmer) by incubation at 60°C overnight; and decolorized by addition of 0.2 mL of 30% hydrogen peroxide. The ^{3}H radioactivity in each sample was measured by scintillation counting. Values were calculated as the percentage of the injected dose per gram (%ID/g) and expressed as mean ± SEM (n = 8). Pharmacokinetic analyses were performed using classical techniques and Phoenix WinNonlin 6.3 software (Pharsight Corp., St. Louis, MO). The CPA-LLP blood concentration-time data were interpreted by non-compartmental methods. The total area under the blood concentration-time curve from zero to the last sampling point and from zero to infinity ($AUC_{0\text{-}\infty}$) and the area under the first moment of the blood concentration-time curve (AUMC) were estimated by the trapezoidal rule with extrapolation of the terminal portion to infinity. The rate constant (K) governing the terminal elimination of CPA-LLP from the body was determined from the least-squares slope of the terminal linear segment of a semi-logarithmic plot of blood CPA-LLP concentration versus time. The elimination half-life was calculated as 0.693/K. The systemic clearance was calculated using the formula Dose/$AUC_{0\text{-}\infty}$. The apparent volume of distribution in the terminal phase was calculated using the formula Dose/[($AUC_{0\text{-}\infty}$)K]. The mean residence time was calculated using the formula AUMC/AUC.

For biodistribution studies, Nu/Nu mice bearing 4T1 tumors were injected intravenously with [^{3}H]CPA-LLP. Mice were euthanized and organs were collected 6 hr after injection. The weight and ^{3}H radioactivity of each organ were recorded. Accumulation of CPA-LLP in each organ was calculated as %ID/g and expressed as mean ± SEM (n = 6).

2.8. Evaluation of antitumor efficacy in mice

After inoculation, mice were maintained for about 7 days (4T1 tumor) or 14 days (Miapaca-2) until the tumor reached about 0.1 cm^3. CPA-LLP was injected via tail vein, and CCPM-^{177}Lu was injected intratumorally. Mice were divided into four groups (n = 8 or 9 per group): (1) control (three injects of saline over one week); (2) CPA-LLP at the equivalent CPA dose of 10 mg/kg per injection, three injections over 1 week; (3) single injection of CCPM-^{177}Lu at 200 μCi per mouse; and (4) CPA-LLP at the equivalent CPA dose of 10 mg/kg per injection, three injections over 1 week, and a single intratumoral injection of CCPM-^{177}Lu at 200 μCi per tumor along with the first dose of CPA-LLP. CCPM-^{177}Lu was given a single injection because of the relatively long half-life of ^{177}Lu (6.7 days). Mouse body weight and tumor volume (1/2 × length × $width^2$) were recorded twice a week. Mice were euthanized once tumor size reached 1200 mm^3. For histologic analysis, tumors were removed, fixed in formalin, embedded in paraffin, sectioned, and stained with hematoxylin-eosin.

2.9. Statistical analysis

Values are expressed as mean ± SEM. Data were evaluated using Student's *t*-test or one-way analysis of variance. A *p* value of less than 0.05 was considered to be statistically significant. Survival curves were analyzed using the Kaplan-Meier method with 95% confidence intervals.

3. Results

3.1. Characteristics of CPA-LLP and CCPM-^{177}Lu

The size of the CPA-LLP in emulsion after homogenization was less than 1 μm, which was further reduced to 48.2 ± 3.1 nm after passage through a microfluidics apparatus (Figure 1B). Transmission electron microscopy confirmed the size and morphology of CPA-LLP (Figure 1C). After passage through a 0.22-μm filter the resultant CPA-LLP dispersion had a CPA concentration of 0.6 mg/mL, while the CPA loading was 0.84% by weight. As shown in Table 1, freezing or lyophilization of CPA-LLP for long-term storage had no significant impact on either CPA size or CPA loading. The release of CPA from CPA-LLP depended on the pH of the incubation buffer (Figure 1D). During incubation at 37°C, 73.2% ± 3.3% of CPA was released by 24 hr in a pH-5.2 buffer, whereas 36.4% ± 2.3% of CPA was released by 24 hr in a pH-7.4 buffer. The total CPA release after 72-hr incubation was 86.1% ± 2.0% for pH 5.2 and 54.9% ± 2.1% for pH 7.4.

The size of CCPM-^{177}Lu was 33.1 ± 1.2 nm, and the radiolabeling efficiency was greater than 95% (Figure S2).

3.2. CPA-LLP inhibited cancer cell proliferation and clonogenicity

CPA-LLP was more toxic than free CPA dissolved in DMSO (Figure 2A and E). The IC_{50} values of CPA-LLP against Miapaca-2 and 4T1 cells were 1.8 ± 0.2 and 2.7 ± 0.2 μM, respectively, whereas the IC_{50} values of free CPA against Miapaca-2 and 4T1 cells were 17.1 ± 1.6 and 11.3 ± 1.2 μM, respectively, 9.5 times and 4.2 times the values for free CPA ($p < 0.0001$). The IC_{50} value of blank LLP was 2.9 mg/mL, which was equivalent to the

amount of LLP in CPA-LLP containing 59 μM of CPA (Figure 2A and S3). Since the IC_{50} concentration of the CPA-LLP formulation is much less than 10 μM CPA, LLP at the concentration equivalent to 10 μM CPA, i.e. ~0.48 mg/mL, should not contribute in any significant way to cell death caused by CPA-LLP. Thus the enhanced cytotoxicity of CPA-LLP was not a contribution of the blank LLP carrier. CPA-LLP also was more effective in preventing colony formation in both cell lines (Figure 2B and F). At the concentration equivalent to 3 μM CPA, CPA-LLP almost completely eliminated cell colonies (Figure 2D and H), while free CPA only reduced colony numbers by 17.7% ± 4.3% in Miapaca-2 cells (Figure 2C) and by 6.7% ± 6.1% in 4T1 cells (Figure 2G).

3.3. CPA-LLP enhanced response of cancer cells to CCPM-^{177}Lu

For the radiosensitization experiments, the starting concentrations of CCPM-^{177}Lu were 0.3, 3, 30, and 300 μCi/ml. The exposure of cells to radiation was calculated to be 0.219, 2.19, 21.9 and 219 μGy, respectively, according to the methods described in Supplemental Materials (Tables S1–3). At all tested doses of CCPM-^{177}Lu, cells treated with CPA-LLP produced significantly fewer colonies than cells not treated with CPA-LLP ($p < 0.05$) (Figure 3). The colony formation efficiency values (%) in Miapaca-2 cells were as follows: 73.1 ± 1.3 vs. 98.1 ± 4.8 at 0.219 μGy, 59.9 ± 2.0 vs. 97.5 ± 3.5 at 2.19 μGy, 49.6 ± 2.0 vs. 66.8 ± 3.1 at 21.9 μGy, and 0.6 ± 0.1 vs. 2.9 ± 0.5 at 219 μGy. Similar trends were observed in 4T1 cells: 73.4 ± 2.3 vs. 89.8 ± 3.2 at 0.219 μGy, 52.1 ± 3.0 vs. 67.9 ± 3.5 at 2.19 μGy, 43.8 ± 2.8 vs. 56.0 ± 2.3 at 21.9 μGy, and 2.4 ± 0.4 vs. 13.9 ± 3.5 at 219 μGy. The formation of Miapaca-2 colonies was not inhibited by blank up to 5 mg/ml CCPM (Figure S4).

3.4. Pharmacokinetics and biodistribution of CPA-LLP

The pharmacokinetics and biodistribution of CPA-LLP were studied using [^{3}H]CPA-LLP. CPA-LLP displayed a bi-exponential disposition following administration, with a fast blood clearance during the first 4 hours and a slower blood clearance thereafter. The %ID/g value in blood decreased from 4.0 ± 0.1 at 0 hr to 1.5 ± 0.1 at 4 hr and 1.1 ± 0.1 at 12 hr (Figure 4A). The pharmacokinetic parameters of CPA-LLP are summarized in Table 2. Of interest, the blood concentration bounced back after 24 hours and remained relatively high through 96 hours after administration of CPA-LLP. This pattern could be attributed to sustained release of CPA from the tissues.

Biodistribution in 4T1-tumor-bearing mice is presented in Figure 4B. The initial blood clearance was accompanied by concomitant uptake of CPA in tumor (Figure 4B): at 6 hr after injection, tumor uptake of CPA-LLP (%ID/g) was 6.0 ± 0.5. The CPA uptakes (%ID/g) in other major organs were as follows: 10.6 ± 0.4 in liver, 2.0 ± 0.3 in spleen, 6.1 ± 0.5 in kidney, 11.6 ± 1.2 in lung, and 13.6 ± 1.3 in intestine.

3.5. CPA-LLP enhanced response of tumor xenografts to CCPM-^{177}Lu

The antitumor efficacy of CPA-LLP, CCPM-^{177}Lu, and the combination against 4T1 xenografts is shown in Figure 5. At day 16 after treatment started, the tumor volume in the monotherapy groups was significantly smaller than that in the non-treatment control group ($p = 0.03$ for CPA-LLP vs. control; $p = 0.04$ for CCPM-^{177}Lu vs. control), and the tumor volume in the combination-therapy group was significantly smaller than the tumor volumes

of control ($p < 0.0001$) and CCPM-^{177}Lu ($p = 0.014$) (Figure 5A). All mice were euthanized at day 18 after the initiation of treatment. Tumor weights were as follows (Figure 5B): control, 1.3 ± 0.1 g; CPA-LLP group, 1.0 ± 0.1 g; CCPM-^{177}Lu group, 0.7 ± 0.1 g; and combination-therapy group, 0.4 ± 0.1 g. The combination-therapy group had significantly lighter tumors than the control ($p < 0.0001$) and CPA-LLP groups ($p = 0.0002$). The body weight of mice did not change significantly during therapy (Figure 5C).

The antitumor efficacy of CPA-LLP, CCPM-^{177}Lu, and the combination against Miapaca-2 xenografts is shown in Figure 6. The combination therapy effectively inhibited tumor growth; tumor volumes with combination therapy were significantly smaller than those in the other groups at all time-points up to 10 days after the initiation of treatment ($p < 0.05$, Figure 6A). The tumor growth curves of individual Miapaca-2 xenografts up to 120 days after the initiation of the treatments from the same study are summarized in Figure S5, and the survival of mice was presented in Figure 6C. The control had significantly shorter survival than all other groups ($p = 0.01$). All 8 mice in the control group died within 3 weeks after treatment started. At the end of the study (day 120), the numbers of surviving mice in the treatment groups were as follows: 3 of 9 mice in the CPA-LLP group, 2 of 9 mice in the CCPM-^{177}Lu group, and 5 of 9 mice in the combination-therapy group. In terms of change in body weight, the combination group showed a reversible 4.7 ± 1.7 % weight loss at day 3, which grew back for later time points (Figure 6B). All other three groups did not have significant weight loss. Representative hematoxylin-eosin-stained tumor sections are shown in Figure 6D–F. Untreated tumors were packed with viable tumor cells (Figure 6D); whereas tumors treated with the combination therapy displayed massive necrosis (Figure 6E, white arrow). The surviving mice in the combination-therapy group were pathologically tumor free (Figure 6F).

4. Discussion

In the present study, we successfully treated both 4T1 and Miapaca-2 tumor xenografts *in vivo* with the combination of CPA formulated as injectable liquid-lipid nanoparticles and β-particle radiation mediated through ^{177}Lu-bound polymeric micelles. To the best of our knowledge, this is the first attempt to achieve combined chemoradiation therapy through two different nanoparticle formulations: one for CPA and one for ^{177}Lu. We successfully loaded CPA into liquid-lipid nanoparticles (~50 nm) that released CPA in a pH-sensitive manner. The pH-responsive CPA release from the liquid-lipid nanoparticles may have been caused by protonation of CPA in acidic pH conditions and subsequent solubilization of protonated CPA. CPA-LLP showed excellent storage stability. All components used in CPA-LLP formulation were safe for clinical use and have been widely employed in formulations for intravenous injection [27, 28]. ^{177}Lu could not be readily formulated in the same liquid-lipid particles with sufficient stability. Therefore, it was attached to nanoparticles through radiometal chelator DTPA, which in turn was covalently conjugated to CCPM. The resulting CCPM-^{177}Lu was directly injected into tumors to achieve localized delivery of radiation. Both *in vitro* and *in vivo* studies showed that the combination therapy not only killed cancer cells but also delayed tumor growth and prevented tumor relapse. Our results suggest that the combination of CPA-LLP and CCPM-^{177}Lu could be an effective treatment for tumors with activated Sonic Hedgehog pathway.

Although CPA has shown promising antitumor properties in many preclinical studies, its insolubility in water posed a substantial obstacle to its clinical translation. A number of approaches have been tried to increase the solubility of CPA in water. For example, several CPA derivatives have been synthesized to incorporate hydrophilic moieties. However, the preparation of such derivatives can be laborious and expensive. Because CPA contains secondary amine, it reacts with acid and thus becomes water soluble. Citric acid and the combination of tartaric acid and cyclodextrin have been used to form complexes with CPA at acidic pH [29]. However, CPA is unstable at acidic pH. Recently, several nanoformulations have been developed to encapsulate CPA. Zhou et al [12] conjugated CPA to poly (N-(2-hydroxypropyl) methacrylamide) via short peptide linker that can be enzymatically cleaved. The resultant conjugate exhibited potency against cancer stem cells. Cho et al [13] loaded CPA into polymeric micelles based on PEG-b-poly(ε-caprolactone) and used this formulation to successfully treat ovarian tumor models. Chitkara et al [14] encapsulated CPA into another customized polymeric micelle formulation for pancreatic cancer therapy.

In the present study, CPA was encapsulated in LLPs consisting of nanodroplets of olive oil stabilized by amphiphilic lipids lecithin S100 and lecithin E80. Our findings showed that CPA-LLP was a promising formulation and deserves further evaluation because of the nontoxic nature of all components used, ease of scaling up production, long shelf-life, and significant antitumor efficacy. All ingredients of LLP are edible and thus should be associated with only minimal risks of toxic effects in patients. CPA was loaded into the oil phase via a microfluidics apparatus. Up to 1 gram of CPA can be easily processed in a couple of hours; thus, the process could be easily scaled up when necessary. The size of LLP was less than 100 nm (Figure 1), which resulted in a prolonged circulation in blood and low uptake in the reticuloendothelial system (Figure 4). CPA-LLP quickly released CPA in acidic buffer (Figure 1D). Since the tumor microenvironment tends to be acidic [30], this pH-dependent release would facilitate CPA accumulation in tumor tissues. CPA-LLP had excellent stability in terms of shelf-life. Once frozen at −80°C or lyophilized, CPA-LLP could be stored without changes in size or CPA loading up to 40 days. Lyophilized CPA-LLP was easily reconstituted by adding water, giving a dispersed solution with nanoparticles similar to freshly prepared CPA-LLP (Table 1). *In vitro* evaluation showed that CPA-LLP had higher cytotoxicity than free CPA. CPA-LLP also was more effective than free CPA in inhibiting the colony formation of both 4T1 and Miapaca-2 tumor cells (Figure 3). *In vivo* pharmacokinetic data showed that CPA-LLP had a prolonged blood circulation and a sustained release of encapsulated CPA over time (Figure 4A). The tumor uptake of 6.0 ± 0.5 %ID/g at 6 hr (Figure 4B) could be attributed to the enhanced permeability and retention effect, which is characteristic of long-circulating nanoformulations.

In the present study, we conjugated ^{177}Lu to the CCPM platform and thus formulated a nanosource of radiation. CCPM can be readily prepared at multiple-gram scale. CCPM has also been tested as a platform for nuclear imaging tracers and demonstrated impressive tumor uptake via the enhanced permeability and retention effect [25]. In the present study, CCPM-^{177}Lu was injected into tumor to precisely control the radiation dose and simplify the interpretation of results. The localized radiation also prevented damage to other vital organs

to minimize possible adverse effects. It is also possible to develop targeted CCPM-^{177}Lu by tagging tumor-homing ligands to the surface of CCPM for internal radiation therapy after systemic administration [31, 32].

CPA is known to sensitize tumors to radiation therapy, which is an important treatment option for cancer, especially for tumors not amenable to surgery. Activation of the Hedgehog pathway protects tumor cells against radiation, while inhibition of the Hedgehog pathway could enhance the tumor response to radiation [33, 34]. The mechanisms underlying radiosensitization by CPA include redistribution of cell cycles to the more ionizing-radiation-sensitive phases, depletion of tumor stem cells, and disruption of DNA-damage repair [35–37]. In the present study, we first evaluated the combination of CPA-LLP and CCPM-^{177}Lu using clonogenic assay (Figure 3). In both 4T1 and Miapaca-2 cells, CPA-LLP enhanced the efficacy of ^{177}Lu radiation therapy by preventing formation of colonies by treated cells. Animal studies confirmed that monotherapy with CPA-LLP or CCPM-^{177}Lu significantly slowed tumor growth in both xenograft models (Figures 5A and 6A). Furthermore, combination therapy slowed tumor growth more than monotherapy did in both xenograft models (Figures 5A **and** 6A).

The limitations of the current study are as follows. First, intratumoral injection of CCPM-^{177}Lu may not be directly applicable in clinical setting. However, we note that brachytherapy, where a sealed radiation source is placed inside or next to the tumor, is commonly used as an effective treatment for cervical, prostate, breast, and other solid tumors. In the current study, CCPM-^{177}Lu was used to test the idea of nanoparticle-immobilized ^{177}Lu as a source of local radiation, either used alone or in combination with CPA-LLP. Our results showed that CCPM-^{177}Lu was effective when delivered intratumorally. These results support designing and testing next generation CCPM-^{177}Lu that can be selectively delivered to the tumor with minimal retention in normal organs after intravenous injection. Second, we used subcutaneous tumor models. In future studies, more clinically relevant pancreatic cancer models, including orthotopic models, genetically engineered mouse models of pancreatic cancer, and human tumor implant models, will be used to further evaluate the antitumor efficacy of CPA-LLP in combination with radiotherapy. Third, in the current study, gross toxicity was estimated by measuring changes in body weight of treated mice. This is by no means adequate. A comprehensive toxicity study is necessary if CPA-LLP and/or CCPM-^{177}Lu were to move towards clinical studies in the future.

5. Conclusion

In summary, we showed that the combination of CPA-LLP and CCPM-^{177}Lu was an effective strategy for cancer therapy in a breast cancer model and a pancreatic cancer model. The CPA-LLP formulation fulfilled several key requirements for drug-delivery systems: biocompatibility, storage stability, and easy scale-up. Localized radiation therapy was achieved by intratumoral injection of CCPM-^{177}Lu to avoid the side effects of whole-body radiation therapy. The effect of chemoradiation therapy was validated by both *in vitro* and *in vivo* studies. Further studies are warranted to investigate the efficacy of the combination of CPA-LLP and external radiotherapy in different breast and pancreatic cancer models,

including drug-resistant and orthotopic models. Studies on the effect of CPA-LLP on radiation-caused DNA damage repair are currently under way.

Supplementary Material

Refer to Web version on PubMed Central for supplementary material.

Acknowledgements

We thank Stephanie Deming for editing the manuscript. This work was supported by the Viragh Family Foundation and the John S. Dunn Foundation. The Research Animal Support and High Resolution Electron Microscopy Facilities are supported by a Cancer Center Support Grant from the National Institutes of Health (P30CA016672).

The funding sources were not involved in study design; in the collection, analysis, and interpretation of data; in the writing of the report; or in the decision to submit the article for publication.

References

1. di Magliano MP, Hebrok M. Hedgehog signalling in cancer formation and maintenance. Nat Rev Cancer. 2003; 3:903–911. [PubMed: 14737121]
2. Kubo M, Nakamura M, Tasaki A, Yamanaka N, Nakashima H, Nomura M, Kuroki S, Katano M. Hedgehog signaling pathway is a new therapeutic target for patients with breast cancer. Cancer Research. 2004; 64:6071–6074. [PubMed: 15342389]
3. Thayer SP, di Magliano MP, Heiser PW, Nielsen CM, Roberts DJ, Lauwers GY, Qi YP, Gysin S, Castillo CF-d, Yajnik V, Antoniu B, McMahon M, Warshaw AL, Hebrok M. Hedgehog is an early and late mediator of pancreatic cancer tumorigenesis. Nature. 2003; 425:851–856. [PubMed: 14520413]
4. Ma X, Sheng T, Zhang Y, Zhang X, He J, Huang S, Chen K, Sultz J, Adegboyega PA, Zhang H, Xie J. Hedgehog signaling is activated in subsets of esophageal cancers. International Journal of Cancer. 2006; 118:139–148.
5. Sirab N, Terry S, Giton F, Caradec J, Chimingqi M, Moutereau S, Vacherot F, de la Taille A, Kouyoumdjian JC, Loric S. Androgens regulate Hedgehog signalling and proliferation in androgen-dependent prostate cells. International Journal of Cancer.
6. Weiner HL, Bakst R, Hurlbert MS, Ruggiero J, Ahn E, Lee WS, Stephen D, Zagzag D, Joyner AL, Turnbull DH. Induction of medulloblastomas in mice by sonic hedgehog, independent of Gli1. Cancer Research. 2002; 62:6385–6389. [PubMed: 12438220]
7. Saito RA, Micke P, Paulsson J, Augsten M, Pena C, Jonsson P, Botling J, Edlund K, Johansson L, Carlsson P, Jirstrom K, Miyazono K, Ostman A. Forkhead box F1 regulates tumor-promoting properties of cancer-associated fibroblasts in lung cancer. Cancer Research. 2010; 70:2644–2654. [PubMed: 20233876]
8. Feldmann G, Habbe N, Dhara S, Bisht S, Alvarez H, Fendrich V, Beaty R, Mullendore M, Karikari C, Bardeesy N, Ouellette MM, Yu W, Maitra A. Hedgehog inhibition prolongs survival in a genetically engineered mouse model of pancreatic cancer. Gut. 2008; 57:1420–1430. [PubMed: 18515410]
9. Feldmann G, Fendrich V, McGovern K, Bedja D, Bisht S, Alvarez H, Koorstra JB, Habbe N, Karikari C, Mullendore M, Gabrielson KL, Sharma R, Matsui W, Maitra A. An orally bioavailable small-molecule inhibitor of Hedgehog signaling inhibits tumor initiation and metastasis in pancreatic cancer. Mol Cancer Ther. 2008; 7:2725–2735. [PubMed: 18790753]
10. Feldmann G, Dhara S, Fendrich V, Bedja D, Beaty R, Mullendore M, Karikari C, Alvarez H, Iacobuzio-Donahue C, Jimeno A, Gabrielson KL, Matsui W, Maitra A. Blockade of hedgehog signaling inhibits pancreatic cancer invasion and metastases: a new paradigm for combination therapy in solid cancers. Cancer Res. 2007; 67:2187–2196. [PubMed: 17332349]

11. Bar EE, Chaudhry A, Lin A, Fan X, Schreck K, Matsui W, Piccirillo S, Vescovi AL, DiMeco F, Olivi A, Eberhart CG. Cyclopamine-mediated hedgehog pathway inhibition depletes stem-like cancer cells in glioblastoma. Stem Cells. 2007; 25:2524–2533. [PubMed: 17628016]
12. Zhou Y, Yang J, Kopecek J. Selective inhibitory effect of HPMA copolymer-cyclopamine conjugate on prostate cancer stem cells. Biomaterials. 2012; 33:1863–1872. [PubMed: 22138033]
13. Cho H, Lai TC, Kwon GS. Poly(ethylene glycol)-block-poly(epsilon-caprolactone) micelles for combination drug delivery: evaluation of paclitaxel, cyclopamine and gossypol in intraperitoneal xenograft models of ovarian cancer. J Control Release. 2013; 166:1–9. [PubMed: 23246471]
14. Chitkara D, Singh S, Kumar V, Danquah M, Behrman SW, Kumar N, Mahato RI. Micellar Delivery of Cyclopamine and Gefitinib for Treating Pancreatic Cancer. Molecular Pharmaceutics. 2012; 9:2350–2357. [PubMed: 22780906]
15. Hermann PC, Huber SL, Herrler T, Aicher A, Ellwart JW, Guba M, Bruns CJ, Heeschen C. Distinct Populations of Cancer Stem Cells Determine Tumor Growth and Metastatic Activity in Human Pancreatic Cancer. Cell Stem Cell. 2007; 1:313–323. [PubMed: 18371365]
16. Mueller MT, Hermann PC, Witthauer J, Rubio Viqueira B, Leicht SF, Huber S, Ellwart JW, Mustafa M, Bartenstein P, D'Haese JG, Schoenberg MH, Berger F, Jauch KW, Hidalgo M, Heeschen C. Combined Targeted Treatment to Eliminate Tumorigenic Cancer Stem Cells in Human Pancreatic Cancer. Gastroenterology. 2009; 137:1102–1113. [PubMed: 19501590]
17. Shafaee Z, Schmidt H, Du W, Posner M, Weichselbaum R. Cyclopamine increases the cytotoxic effects of paclitaxel and radiation but not cisplatin and gemcitabine in Hedgehog expressing pancreatic cancer cells. Cancer Chemotherapy and Pharmacology. 2006; 58:765–770. [PubMed: 16552573]
18. Vera DR, Eigner S, Henke KE, Lebeda O, Melichar F, Beran M. Preparation and preclinical evaluation of 177Lu-nimotuzumab targeting epidermal growth factor receptor overexpressing tumors. Nuclear Medicine and Biology. 2012; 39:3–13. [PubMed: 21958849]
19. Pan MH, Gao DW, Feng J, He J, Seo Y, Tedesco J, Wolodzko JG, Hasegawa BH, Franc BL. Biodistributions of 177Lu- and 111In-labeled 7E11 antibodies to prostate-specific membrane antigen in xenograft model of prostate cancer and potential use of 111In-7E11 as a pre-therapeutic agent for 177Lu-7E11 radioimmunotherapy. Mol Imaging Biol. 2009; 11:159–166. [PubMed: 19034582]
20. Baum RP, Kulkarni HR. THERANOSTICS: From Molecular Imaging Using Ga-68 Labeled Tracers and PET/CT to Personalized Radionuclide Therapy - The Bad Berka Experience. Theranostics. 2012; 2:437–447. [PubMed: 22768024]
21. Sundberg AL, Gedda L, Orlova A, Bruskin A, Blomquist E, Carlsson J, Tolmachev V. [Lu-177]Bz-DTPA-EGF: preclinical characterization of a potential radionuclide targeting agent against glioma. Cancer Biotherapy and Radiopharmaceuticals. 2004; 19:195–204. [PubMed: 15186600]
22. Dumont RA, Tamma M, Braun F, Borkowski S, Reubi JC, Maecke H, Weber WA, Mansi R. Targeted radiotherapy of prostate cancer with a gastrin-releasing peptide receptor antagonist is effective as monotherapy and in combination with rapamycin. Journal of Nuclear Medicine. 2013; 54:762–769. [PubMed: 23492884]
23. Heller E, Hurchla MA, Xiang J, Su X, Chen S, Schneider J, Joeng KS, Vidal M, Goldberg L, Deng H, Hornick MC, Prior JL, Piwnica-Worms D, Long F, Cagan R, Weilbaecher KN. Hedgehog signaling inhibition blocks growth of resistant tumors through effects on tumor microenvironment. Cancer Research. 2012; 72:897–907. [PubMed: 22186138]
24. Tsuda N, Ishiyama S, Li Y, Ioannides CG, Abbruzzese JL, Chang DZ. Synthetic microRNA designed to target glioma-associated antigen 1 transcription factor inhibits division and induces late apoptosis in pancreatic tumor cells. Clinical Cancer Research. 2006; 12:6557–6564. [PubMed: 17085671]
25. Zhao J, Song S, Zhong M, Li C. Dual-Modal Tumor Imaging via Long-Circulating Biodegradable Core-Cross-Linked Polymeric Micelles. ACS Macro Letters. :150–153.
26. Franken NAP, Rodermond HM, Stap J, Haveman J, van Bree C. Clonogenic assay of cells in vitro. Nat. Protocols. 2006; 1:2315–2319.

27. Tomsits E, Pataki M, Tolgyesi A, Fekete G, Rischak K, Szollar L. Safety and efficacy of a lipid emulsion containing a mixture of soybean oil, medium-chain triglycerides, olive oil, and fish oil: a randomised, double-blind clinical trial in premature infants requiring parenteral nutrition. Journal of Pediatric Gastroenterology and Nutrition. 2010; 51:514–521. [PubMed: 20531018]
28. Davis SS, Washington C, West P, Illum L, Liversidge G, Sternson L, Kirsh R. Lipid emulsions as drug delivery systems. Annals of the New York Academy of Sciences. 1987; 507:75–88. [PubMed: 3327420]
29. Quint E, Smith A, Avaron F, Laforest L, Miles J, Gaffield W, Akimenko M-Ae. Bone patterning is altered in the regenerating zebrafish caudal fin after ectopic expression of sonic hedgehog and bmp2b or exposure to cyclopamine. Proceedings of the National Academy of Sciences. 2002; 99:8713–8718.
30. Neesse A, Michl P, Frese KK, Feig C, Cook N, Jacobetz MA, Lolkema MP, Buchholz M, Olive KP, Gress TM, Tuveson DA. Stromal biology and therapy in pancreatic cancer. Gut. 60:861–868. [PubMed: 20966025]
31. Zhang R, Lu W, Wen X, Huang M, Zhou M, Liang D, Li C. Annexin A5-conjugated polymeric micelles for dual SPECT and optical detection of apoptosis. Journal of Nuclear Medicine. 2011; 52:958–964. [PubMed: 21571801]
32. Zhang R, Xiong C, Huang M, Zhou M, Huang Q, Wen X, Liang D, Li C. Peptide-conjugated polymeric micellar nanoparticles for dual SPECT and optical imaging of EphB4 receptors in prostate cancer xenografts. Biomaterials. 2011; 32:5872–5879. [PubMed: 21612822]
33. Sims-Mourtada J, Izzo JG, Apisarnthanarax S, Wu TT, Malhotra U, Luthra R, Liao Z, Komaki R, van der Kogel A, Ajani J, Chao KS. Hedgehog: an attribute to tumor regrowth after chemoradiotherapy and a target to improve radiation response. Clinical Cancer Research. 2006; 12:6565–6572. [PubMed: 17085672]
34. Chen YJ, Lin CP, Hsu ML, Shieh HR, Chao NK, Chao KS. Sonic hedgehog signaling protects human hepatocellular carcinoma cells against ionizing radiation in an autocrine manner. Int J Radiat Oncol Biol Phys. 2011; 80:851–859. [PubMed: 21377281]
35. Wu XY, Che J, Sun KK, Shen XJ, Yang D, Zhong N, Zhao H. Cyclopamine increases the radiosensitivity of human pancreatic cancer cells by regulating the DNA repair signal pathway through an epidermal growth factor receptordependent pathway. Mol Med Rep. 2013; 8:979–983. [PubMed: 23903906]
36. Zeng J, Aziz K, Chettiar ST, Aftab BT, Armour M, Gajula R, Gandhi N, Salih T, Herman JM, Wong J, Rudin CM, Tran PT, Hales RK. Hedgehog pathway inhibition radiosensitizes non-small cell lung cancers. Int J Radiat Oncol Biol Phys. 2013; 86:143–149. [PubMed: 23182391]
37. Che J, Zhang FZ, Zhao CQ, Hu XD, Fan SJ. Cyclopamine is a novel Hedgehog signaling inhibitor with significant anti-proliferative, anti-invasive and anti-estrogenic potency in human breast cancer cells. Oncol Lett. 2013; 5:1417–1421. [PubMed: 23599805]

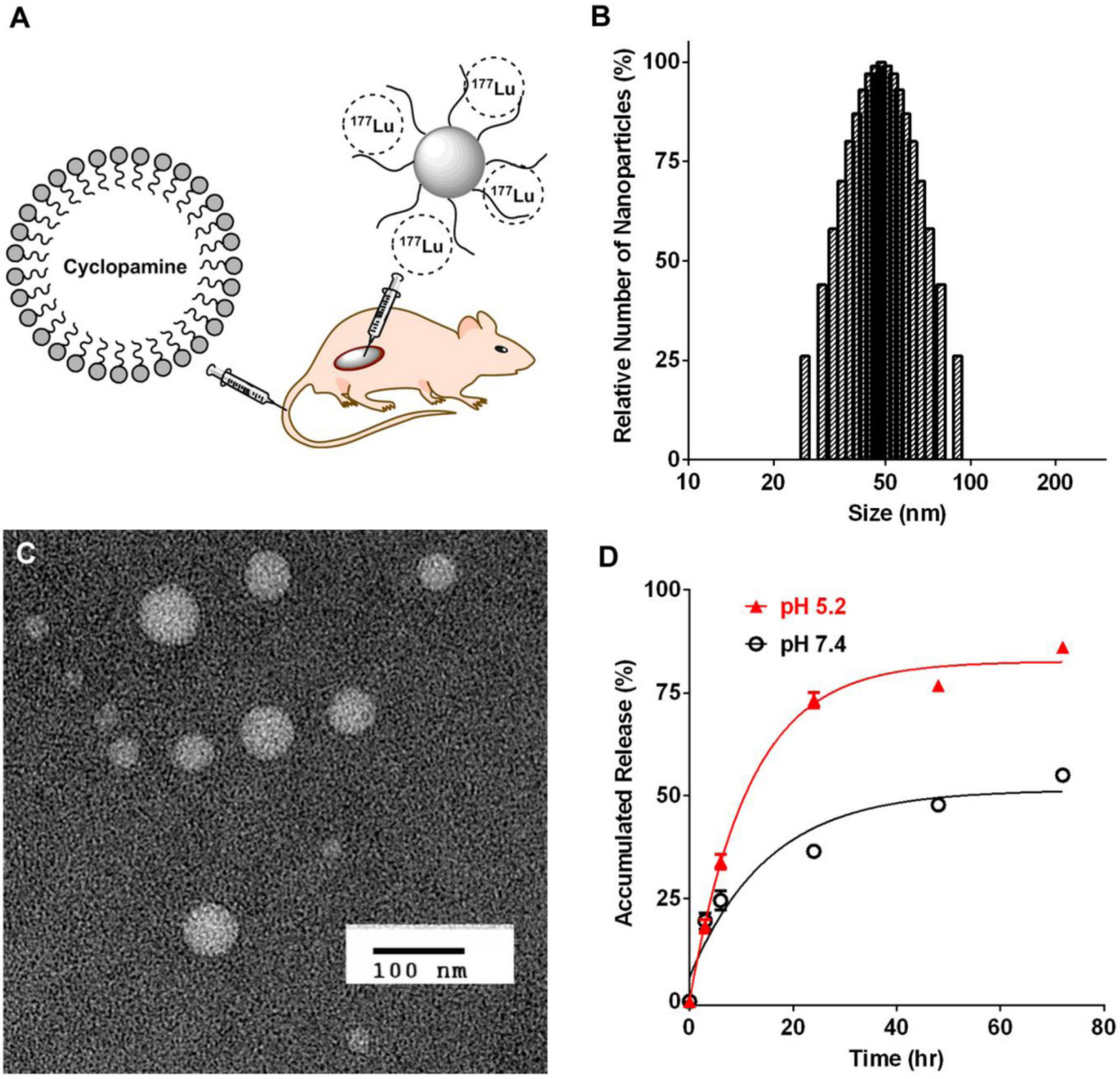

Figure 1.

(A) Schematic illustration of study design. Radioactive polymeric micelles containing ^{177}Lu were injected intratumorally, and CPA-loaded lipid nanoparticles were injected intravenously. (B-D) Characterization of CPA-LLP. (B) Dynamic light scattering histogram of CPA-LLP. (C) Transmission electron microscopy images of CPA-LLP (negative staining). (D) Profile of CPA release from CPA-LLP at 37°C in pH-5.2 and pH-7.4 buffers. Data are plotted as accumulated release (%) relative to total CPA payload and presented as mean ± SEM (n = 3).

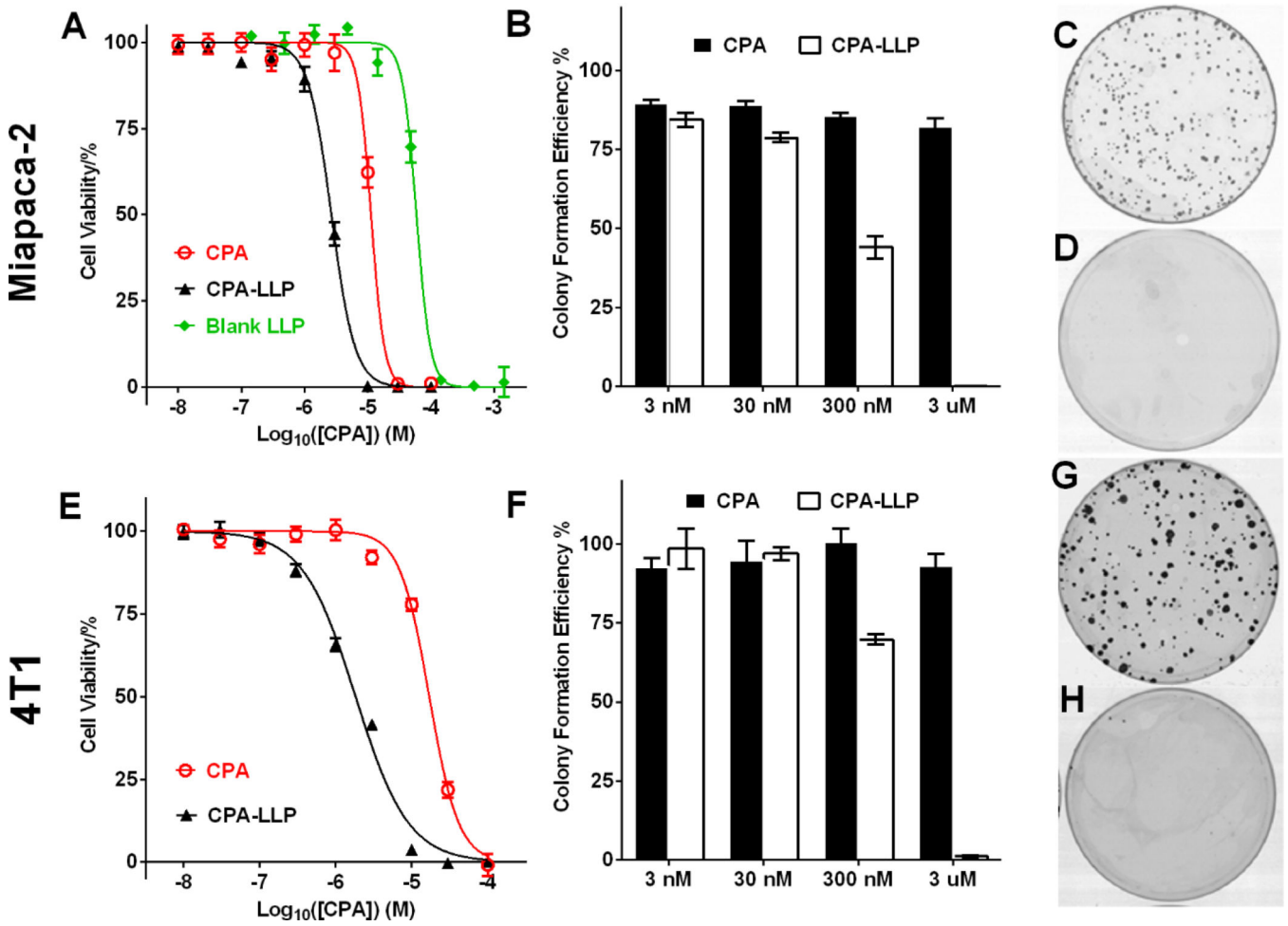

Figure 2.

Viability and colony formation of Miapaca-2 (A-D) and 4T1 cells (E-H) after treatment with CPA-LLP. (A and E) Cell viability after 96-hr treatment with CPA-LLP. The concentration of blank LLP was equal to the concentrations of LLP in corresponding CPA-LLP. Data are normalized to non-treatment control and presented as mean ± SEM (n = 6). (B and F) Efficiency of colony formation after treatment with each drug for 7 days. Data are normalized to non-treatment control and presented as mean ± SEM (n = 4). (C and G) Representative photographs of cell colonies after treatment with free CPA (3 μM). (D and H) Representative photographs of cell colonies after treatment with CPA-LLP at a concentration equivalent to 3 μM CPA.

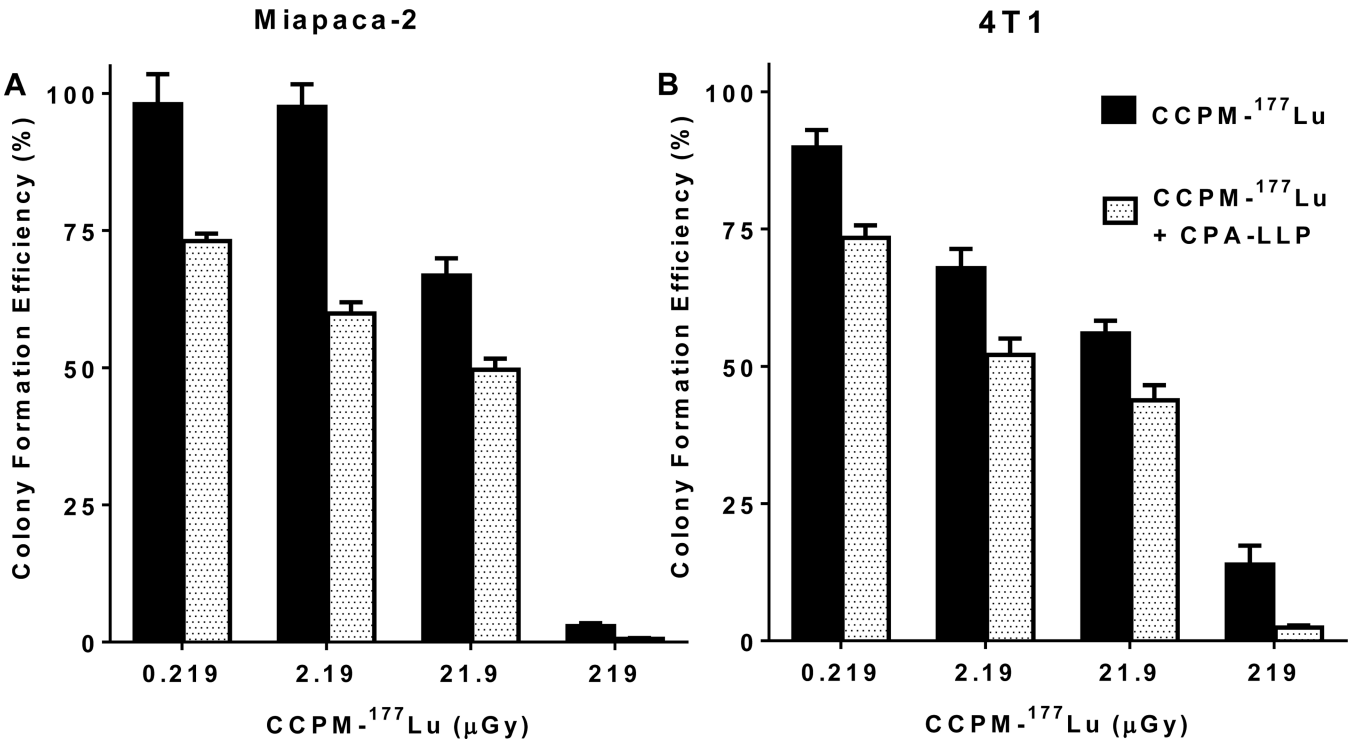

Figure 3.

Efficiency of colony formation of Miapaca-2 (A) and 4T1 (B) cells after treatment with CCPM-^{177}Lu alone or in combination with CPA-LLP. Cells at 70% confluence were treated with CCPM-^{177}Lu at escalating doses with or without CPA-LLP (10 μM equivalent CPA) for 24 hr, and then colony formation was assessed. Data are plotted as colony formation efficiency relative to that of nontreatment control and are presented as mean ± SEM (n = 4). At each dose of CCPM-^{177}Lu, the presence of 10-μM CPA-LLP caused a significant decrease in colony formation efficiency ($p < 0.05$).

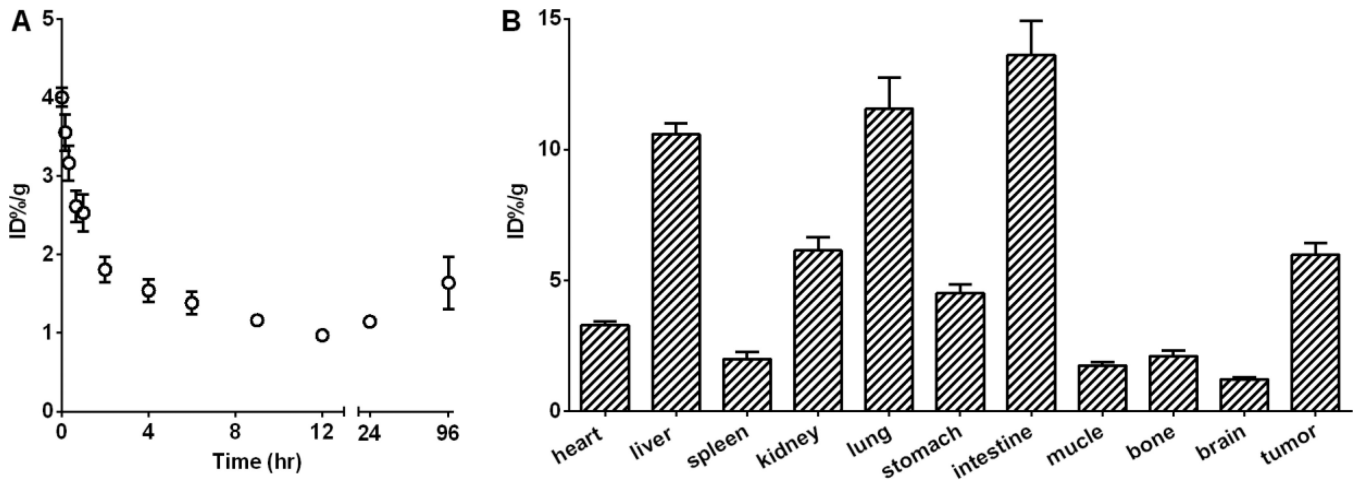

Figure 4.

Pharmacokinetic and biodistribution studies of [H^3]CPA-LLP. (A). Blood activity-time profile. Open circles represent radioactivity expressed as percentage of injected dose per gram of blood (%ID/g) (n = 8). (B) Biodistribution results obtained from radioactivity counting in organs of mice sacrificed 6 hr after injection (n = 6). All data are expressed as mean ± SEM.

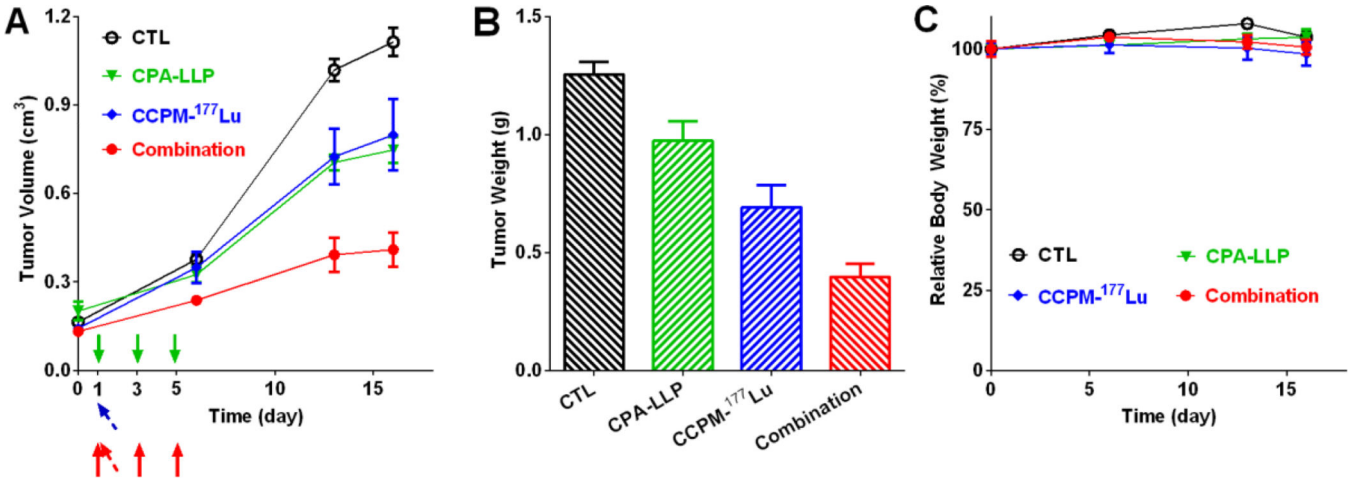

Figure 5.

Antitumor efficacy of CPA-LLP and CCPM-^{177}Lu against 4T1 xenografts. (A) Tumor growth curves. The injections of CPA-LLP are marked by solid arrow (green for the CPA-LLP monotherapy group, red for the combination group). The injection of CCPM-^{177}Lu is marked by tilted arrow (blue for the CCPM-^{177}Lu monotherapy group, red for the combination group). On day 16, the tumor volume in the mono-therapy groups was significantly smaller than that in the non-treatment control group ($p = 0.03$ for CPA-LLP vs. control; $p = 0.04$ for CCPM-^{177}Lu vs. control), and the tumor volume in the combination-therapy group was significantly smaller than the tumor volumes of control ($p < 0.0001$) and CCPM-^{177}Lu ($p = 0.014$). (B) Tumor weights at end of study (day 18 after the start of treatment). The combination-therapy group had significantly lighter tumors than the control ($p < 0.0001$) and CPA-LLP groups ($p = 0.0002$) (C) Relative change in body weight during treatment. All data are expressed as mean ± SEM (n = 9).

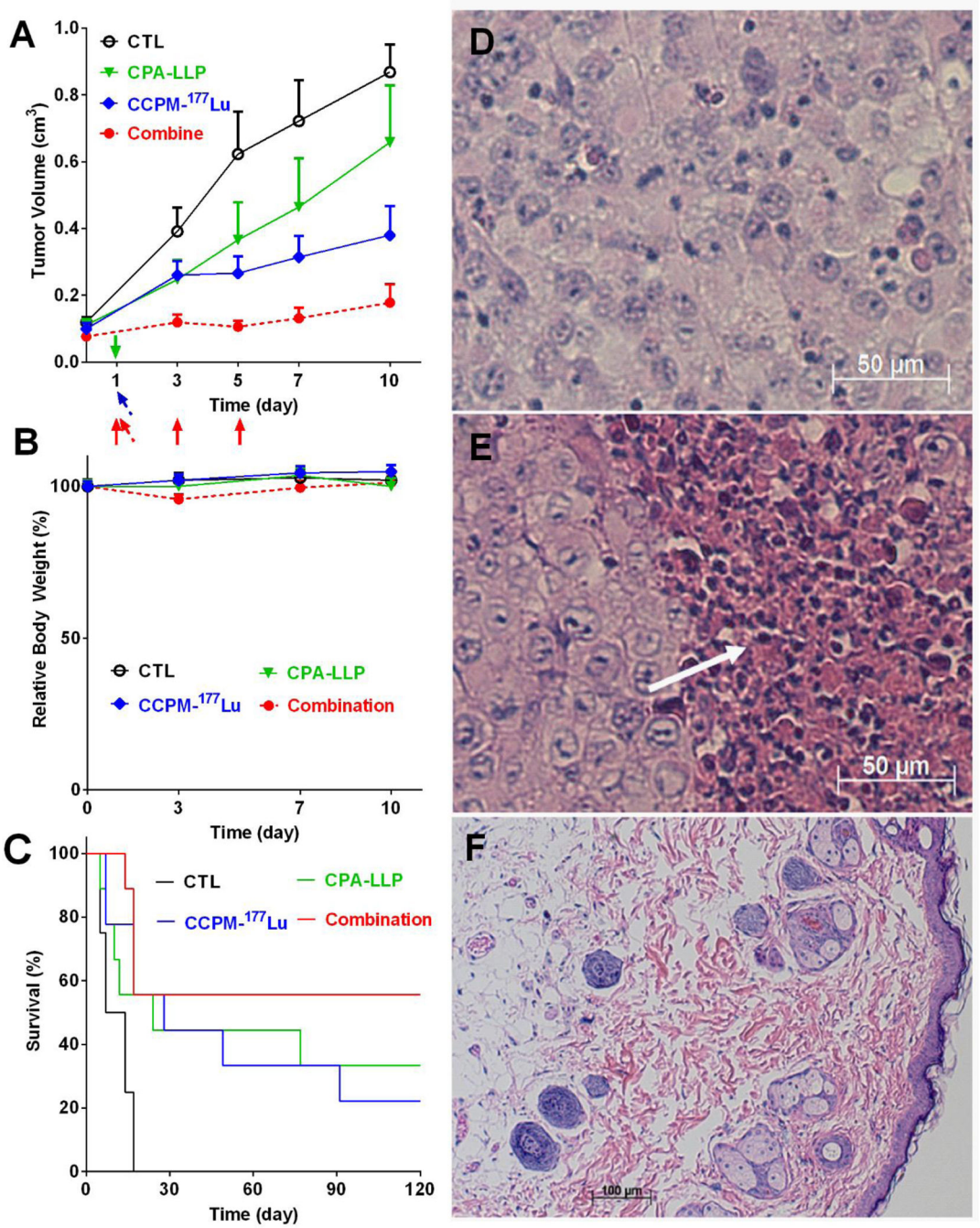

Figure 6.

Antitumor efficacy of CPA-LLP and CCPM-^{177}Lu against Miapaca-2 xenografts (n = 8 or 9). (A) Tumor growth curves. The injections of CPA-LLP are marked by solid arrow (green for the CPA-LLP monotherapy group, red for the combination group). The injections of CCPM-^{177}Lu are marked by tilted arrow (blue for the CCPM-^{177}Lu monotherapy group, red for the combination group). Data are expressed as mean ± SEM. The combination therapy effectively inhibited tumor growth; tumor volumes with combination therapy were significantly smaller than those in the other groups at all time-points at which tumor volume

was measured ($p < 0.05$). (B) Relative change in body weight during treatment. All data are expressed as mean ± SEM (n = 9). (C) Mouse survival curves. The non-treatment control had significantly shorter survival than all other three groups ($p = 0.01$). (D-F) Representative photomicrographs of hematoxylin-eosin-stained tumor slices. (D) Tumor from control group. (E) Residual tumor from combination-therapy group. White arrow indicates necrotic region. (F) Scar tissue at tumor inoculation site from combination-therapy group.

Table 1

Effect of freezing or lyophilization for long-term storage on CPA-LLP size and drug loading

Characterization	Original	After 40 days at 4°C	After reconstitution from lyophilized powder
Intensity-average size (nm)	90.3 ± 1.5	85.7 ± 3.4	96.2 ± 2.1
Relative CPA loading (%)	100	92.3	103.2

Table 2

Pharmacokinetic parameters for CPA-LLP

Parameter	Mean ± standard deviation
C_{max} (%ID/g)	4.05 ± 0.38
AUC_{Last} (%ID· h/g)	131.6 ± 35.3
$AUC_{0-\infty}$ (%ID· h/g)	147.0 ± 36.0
Terminal elimination half-life (h)	9.94 ± 3.4
Systemic clearance (g/h)	0.7089 ± 0.141
V_z (g)	9.96 + 3.4
Mean residence time (h)	58.0 ± 6.3

C_{max}, predicted maximum blood concentration; AUC_{Last}, area under the blood concentration curve from zero to the last sampling point; $AUC_{0-\infty}$, area under the blood concentration curve from zero to infinity; V_Z, apparent volume of distribution in the terminal phase.